SIMULATION AND EXPERIMENT OF MONORAIL ANTI-FROST MACHINE IN HILLY ORCHARD
/
丘陵山地果园单轨式防霜机的仿真与试验

Qingfu GONG [1)], Yuepeng SONG[1,2)], Wei MA[3)], Hongmei ZHANG [1)], Xiang HAN[1)], Ang GAO [1)], Longlong REN [1,2*)]
[1)] Shandong Agricultural University, College of Mechanical and Electrical Engineering/ China;
[2)] Shandong Provincial Engineering Laboratory of Agricultural Equipment Intelligence/ China;
[3)] Institute of Urban Agriculture, Chinese Academy of Agricultural Sciences/ China
E-mail: renlonglong@sdau.edu.cn
DOI: https://doi.org/10.35633/inmateh-72-14

Keywords: *Frost; Frost protection wind machine; Hilly Orchard; Fluent; Simulation; Diffusion*

ABSTRACT
In order to solve the problems of artificial operation, high labor intensity and low efficiency of frost prevention in hilly orchards, this study focused on hilly orchards and designed a smoke frost prevention machine based on the agronomic requirements for frost prevention in hilly orchards. Utilizing Fluent software, a simulation analysis was conducted on the spatiotemporal distribution characteristics of smoke mass concentration and temperature during the smoke diffusion process based on the discrete phase model. The results indicated continuous emission of smoke at a velocity of 6 m/s, with smoke plume volume gradually increasing and reaching a stable diffusion state after 9 seconds. Based on the established smoke diffusion simulation model, an orthogonal experimental analysis of the working parameters at the smoke outlet of the frost prevention machine was conducted using the warming amplitude near the canopy as an index. The optimal combination of working parameters at the smoke outlet was determined to be a smoke outlet velocity of 6 m/s, a smoke outlet angle of 60°, and a smoke outlet diameter of 140 mm. The field experiments demonstrated that the frost prevention machine operating at a speed of 0.6 m/s continuously for 0.5 hours could increase the temperature within the range of 1.5 m to 4 m above ground level by approximately 1.7°C. This research is of great significance to reduce the frost disaster loss of hilly orchards and improve the economic benefits of hilly orchards.

摘要
为了解决丘陵果园防霜以人工作业为主、劳动强度大、作业效率低的问题，本文以丘陵果园为研究对象，基于丘陵果园防霜冻的农艺要求，设计了一种基于丘陵果园输运轨道的烟雾防霜机。借助 Fluent 软件，基于离散相模型对烟雾扩散过程中烟雾质量浓度和温度的时空分布特性进行仿真分析，结果表明烟雾以 6 m/s 的速度持续喷发，烟羽体积逐渐增大，9s 后，烟雾达到稳定扩散状态；基于建立的烟雾扩散仿真模型，以果树冠层附近的增温幅度为指标，对防霜机烟雾出口处的工作参数进行正交试验分析，结果表明防霜机烟雾出口处的工作参数最佳组合为烟雾出口速度为 6m/s，烟雾出口角度为 60°，烟雾出口直径为 140 mm。田间试验结果表明，防霜机以 0.6 m/s 的运行速度连续作业 0.5 h，可将工作区域 1.5 m 至 4 m 高度范围内的温度升高约 1.7° C。该研究对降低丘陵果园霜冻灾害损失，提升丘陵果园经济效益具有重要意义。

INTRODUCTION
In recent years, extreme weather such as frost caused by spring low temperatures has occurred frequently *(Ferrez et al., 2011)*. Affected by the geographical environment, frost damage caused by low temperatures has become one of the main natural disasters. Frost damage caused by low temperatures often occurs during the flowering period of fruit trees. If there are no effective protective measures, it is easy to cause a large-scale production reduction or even extinction, which brings serious economic losses to fruit farmers *(Li et al., 2018; Zhang et al., 2019)*.

Frost prevention in the orchard is not only a crucial method for addressing frost disasters but also a key aspect in managing the flowering period of fruit tree *(Ran et al., 2020)*. Research on anti-frost technology of orchards is relatively early and mature. Mechanized frost prevention has become an important technical means to prevent frost *(Beyá-Marshall et al., 2019)*. At present, the domestic frost protection measures in orchards are mainly based on traditional frost prevention methods such as artificial flooding, chemical whitening of the tree trunks, smoke and tree canopy covering. The problems of consuming a significant amount of time and energy and wasting resources have seriously affected the sustainable and healthy development

of the fruit industry *(Dai et al., 2009)*. Therefore, mechanized frost prevention operations will play a crucial role in protecting orchards from frost. At present, foreign research on anti-frost machines is relatively early. There are many types of anti-frost machines in foreign countries and the degree of mechanization is relatively high *(Augspurger, 2013)*. According to the principle of anti-frost, anti-frost machines mainly include air-assisted anti-frost machines, suction-exhaust anti-frost machines, anti-frost helicopters, and warm-wind anti-frost machines *(Reese et al., 1969; Mikio et al., 2007; Vincent et al., 2020; Yazdanpanah et al., 2011; Battany, 2012; Poling, 2008; Hu et al., 2015)*.

The existing anti-frost machines are dedicated to special machines and have a single function, which results in a low utilization rate and a high idle rate. The low utilization rate of agricultural machines is one of the important reasons for the increase in the cost of agricultural machines and the difficulty in the promotion and application of agricultural machines *(Zhang et al., 2016)*. Therefore, in order to reduce the idle power equipment of agricultural machinery, the design of the anti-frost machine in hilly orchards should adopt the method of combining agricultural machines and power equipment in the hilly orchard to realize the anti-frost working. According to the developing status of domestic hilly orchard power machinery, it can be known that the hilly orchard transportation track tractor which has strong transportation capacity, small and exquisite structure design *(Liu., 2018; Yan et al., 2023; Song et al., 2017)*, and the ability to overcome terrain obstacles is the best choice for the power equipment of anti-frost machine in the hilly orchard.

According to the agronomic requirements for frost protection in hilly orchards, a smoke anti-frost machine based on the monorail transport track of hilly orchards, which reduces the frost disasters and the economic losses of orchards, was developed. The smoke anti-frost machine developed in combination with the existing power equipment of the hilly orchard realizes the mechanized anti-frost working. At the same time, it is of great significance to reduce the cost of frost prevention in orchards and increase the income of fruit growers.

MATERIALS AND METHODS

Whole structure and working principle

Whole structure

Combined with the above analysis, a smoke anti-frost machine based on the transportation track of hilly orchard was designed, as shown in Figure 1.

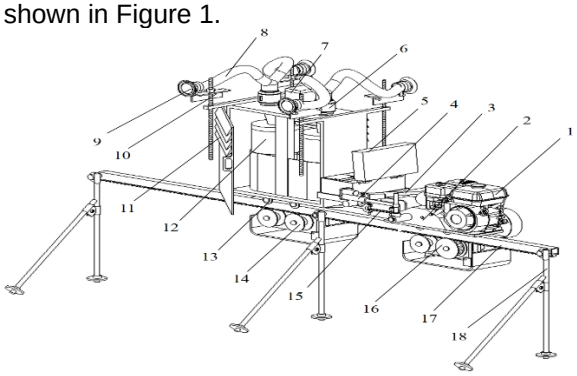

Fig. 1 - Structure diagram of frost protection smoke machine based on transportation track of hilly orchard

1. Gasoline engine; 2. Clutch device; 3.Electric push rod device 1; 4.Electric push rod device 2; 5.Control cabinet; 6.fan; 7.DC power supply box; 8.Hose for transporting smoke; 9.Smoke outlet; 10.Adjusting device for smoke outlet; 11.Vent; 12.Smoke generating agent placement box; 13.Bearing wheel; 14.Guide wheel; 15.Junction device; 16.Drive pin wheel; 17.Track; 18.Support frame

Working principle

The whole structure is mainly composed of the transportation track tractor, the smoke generation and transportation components, and the control cabinet. Smoke generation and transportation components are connected to the transportation track tractor by the junction device. The tractor drives the movement of the smoke transportation components to realize the mobile anti-frost operation in hilly orchards. During the anti-frost operation, the operation of the anti-frost machine is mainly controlled by the electric push rod device.

The smoke generation and transportation components of the anti-frost machine are mainly composed of smoke-generator, fan, and system control components. The control system of smoke generation and transportation components is mainly based on the programmable controller, which completes the generation and output of smoke by controlling the ignition of the smoke-generating agent and the opening and closing of the fan. The smoke-generating agent burns with oxygen to generate highly dispersed oxide particles, which quickly diffuse under the action of the fan and form a large amount of smoke.

Smoke floats in the air at a certain height for a long time, forming a smoke screen. The smoke screen can effectively reduce the heat radiation loss of the soil and fruit trees. At the same time, the large amount of smoke generated dissolves the damp and cold air in the frost orchard into water and releases a certain amount of latent heat, which can effectively increase the temperature of the surrounding environment and achieve the purpose of frost prevention in the orchard.

Main technical parameters

According to the topographical distribution characteristics of hilly orchards in northern China and the design requirements of the planting characteristics of fruit trees on the frost-proof machine, the overall design parameters of the smoke anti-frost machine in hilly orchards were preliminarily determined, as shown in Table 1.

Table 1

Table of main technical parameters

Item	Design parameters of the prototype
Auxiliary Power of tractor	Gasoline engine
Size of the whole machine (length ×width ×height/cm)	160×40×160
Operating speed（m/s）	0.5~1
Remote control distance（m）	≥100
Amplitude of warming when the anti-frost machine works for 0.5 h（℃）	≥1.5

CFD numerical simulation analysis of smoke diffusion based on Fluent

Based on the discrete-phase multi-phase flow model, Fluent software was used to simulate the diffusion process of smoke. The law of smoke diffusion was obtained by analyzing the mass concentration of smoke particles and temporal and spatial distribution characteristics of temperature. At the same time, to explore the influence law of the working parameters of the smoke outlet on the warming magnitude of the orchard environment and provide a theoretical basis for the optimization design of the anti-frost machine, three factors and three levels orthogonal experiment was carried out by selecting the speed of the smoke outlet, the angle of the smoke outlet and the diameter of the smoke outlet as the inspection factors, taking environmental warming amplitude as evaluation index and using discrete phase smoke diffusion model and method of orthogonal experiment.

CFD simulation and numerical model of smoke diffusion

The smoke diffusion process is a typical discrete-phase diffusion model. In view of the fact that airflow and the diffusion movement of smoke particles should be fully considered when establishing the simulation model, the method of combining Euler-Lagrange with coordinates was used to simulate. In the calculation process of the two-phase flow numerical model of the Euler-Lagrange method, the air-fluid was considered as a continuous phase and its flow characteristics under Euler coordinates were studied. In addition, smoke particles were considered as discrete phases and the movement of particles in the flow field over time under Lagrange coordinates was tracked *(Song et al., 2017)*.

(1) Numerical model of air flow

In this paper, the governing equations of turbulent kinetic energy k, turbulent dissipation rate ε, turbulent viscosity μ_t and turbulent time-averaged parameters were established by using Realizable $k-\varepsilon$ turbulence model.

The calculation control equations of k and ε are as follows:

$$\frac{\partial(\rho k)}{\partial t}+\frac{\partial(\rho k\mu_i)}{\partial x_i}=\frac{\partial}{\partial x_j}\left[\left(\mu+\frac{\mu_t}{\sigma_k}\right)\frac{\partial k}{\partial j_k}\right]+G_k-\rho\varepsilon \quad (1)$$

$$\frac{\partial(\rho\varepsilon)}{\partial t}+\frac{\partial(\rho\varepsilon u_i)}{\partial x_i}=\frac{\partial}{\partial x_j}\left[\left(\mu+\frac{\mu_t}{\sigma_\varepsilon}\right)\frac{\partial\varepsilon}{\partial x_j}\right]+C_1\varepsilon\frac{G_k}{k}-C_2\rho\frac{\varepsilon^2}{k} \quad (2)$$

In the above formula, k is the Turbulent kinetic energy; ε is the Turbulent dissipation rate; σ_k is the Turbulent Prandtl number corresponding to turbulent kinetic energy k; σ_ε is the Turbulent Prandtl number corresponding to Turbulent dissipation rate ε; C_1 and C_2 are the Empirical constant; G_k is the Turbulent kinetic energy derived from average velocity gradient.

(2) Numerical model of smoke particles

In the process of solving the two-phase flow discrete phase numerical model based on the Euler-Lagrange coordinate method, the fluid was taken as the continuous phase and the force balance differential equation and trajectory differential equation of the particle were integrated. Finally, the velocity and trajectory of each position of the particle were obtained *(Jian et al., 2020)*. The particle x-axis force balance equation and trajectory equation expression are, respectively:

$$\frac{du_p}{dt} = F_D(v_t - v_p) + (\rho_p - \rho)\frac{g_x}{\rho_p} + F_x \quad (3)$$

$$\frac{dx}{dt} = v_p \quad (4)$$

In the above formula, v_t is the fluid phase velocity in the x-axis direction; v_p is the particle velocity in the x-axis direction; ρ_p is the packing density of particle; F_x is the other forces per unit mass; $F_D(v_t - v_p)$ is the drag function per unit mass of particles.

The fuming agent material selected by the anti-frost machine in the orchard is mainly composed of manganese dioxide, iron trioxide, barium nitrate, and potassium permanganate. The smoke-generating agent will generate tiny solid particles after burning. The particle size of the smoke particles generated by the combustion of smoke-generating agent obeys the Rosin-Rammler distribution *(González-Tello et al., 2008)*. The expression of Rosin-Rammler distribution function is *(Delagarmmatikas et al., 2010)*:

$$F(d) = 1 - \exp[1 - \beta d^n] \quad (5)$$

In the above formula, β is the characteristic parameter; d is the particle size; n is the distribution index; $F(d)$ is the cumulative percentage of particle size less than d.

Establishment of smoke diffusion simulation model

In the simulation analysis of CFD fluid, it is crucial to determine a reasonable calculation domain. The smoke anti-frost machine designed in this paper can perform dynamic cycle operation along the transportation track of hilly orchard. Therefore, the size of the computational domain and the structure of the anti-frost machine should be simplified under the premise of ensuring the reliability of the simulation results when exploring the law of smoke diffusion. The simplified simulation model is: under the condition of airflow velocity of 1 m/s, smoke particles with a certain temperature and velocity are ejected from the smoke outlet and diffuse in the environment; assuming that the vertical height of the smoke outlet from the ground is 1000 mm, the angle of the smoke outlet is 60°, the diameter of the smoke outlet is 100 mm, and the computational domain of the model is a cube of 1000 mm×1000 mm × 1000 mm. At the same time, in order to facilitate the study of the temporal and spatial characteristics of smoke in the flow field, a typical plane of z = 0 was established, as shown in Figure 2 (a).

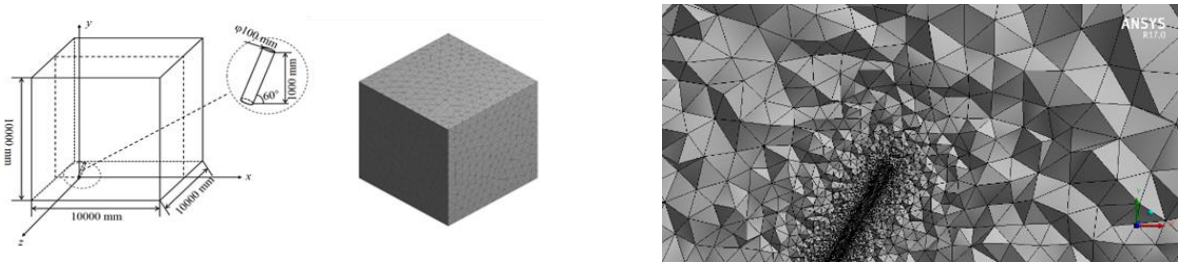

a) Physical model size of computational domain b) Unstructured grid division

Fig. 2 - Computational domain size and unstructured grids generation

RESULTS

Analysis of the smoke diffusion process

Figure 3 (a) ~ (h) are the cloud diagrams of the smoke mass concentration distribution at the typical time within 1 ~ 15 s on the z=0 section. According to Figure 3, it can be seen that as smoke continues to erupt at 6 m/s, smoke diffuses horizontally along the x-axis due to the influence of airflow. The volume of plume (Smoke flow's shape at punctiform emission sources) gradually increased within 1 s - 7 s. The plume had an inverted V shape; with the increase of the eruption time of smoke, the smoke diffusion reached a steady state after 9 s.

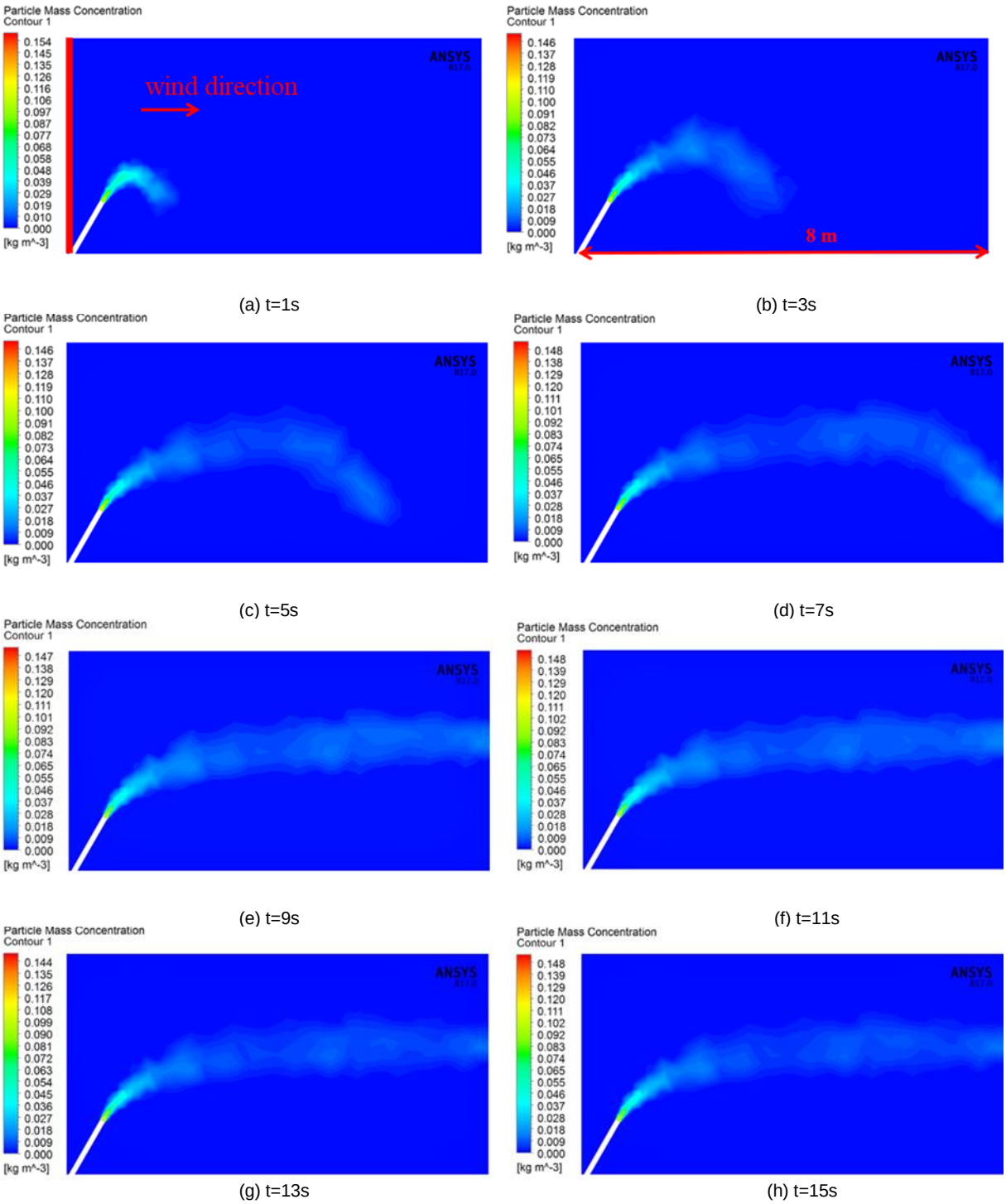

Fig. 3 - Distributions of smoke mass concentration at different times

In order to further study the variation law of smoke mass concentration in the diffusion process of smoke along the x-axis, the center of the bottom of the smoke outlet was taken as the origin of the coordinates, the horizontal distance as the x-axis and the smoke mass concentration at a height of 2 m on the z=0 section as y-axis. Figure 4 shows the variation curve of smoke particle mass concentration. It can be seen from Figure 4 that when x=0, the mass concentration of smoke is 0. As the distance increases, the mass concentration of smoke first increased and then decreased. In the BC section of the curve, the main reason for the increase in smoke mass concentration is that the smoke outlet is 60° to the x-axis. Affected by the direction of wind flow, the diffusion tilt amplitude of the plume gradually decreased, and finally is parallel to the x-axis. In the CD section of the curve, the main reason for the fluctuation of the smoke mass concentration is that the shape of the plume formed during the horizontal diffusion of the smoke is relatively irregular.

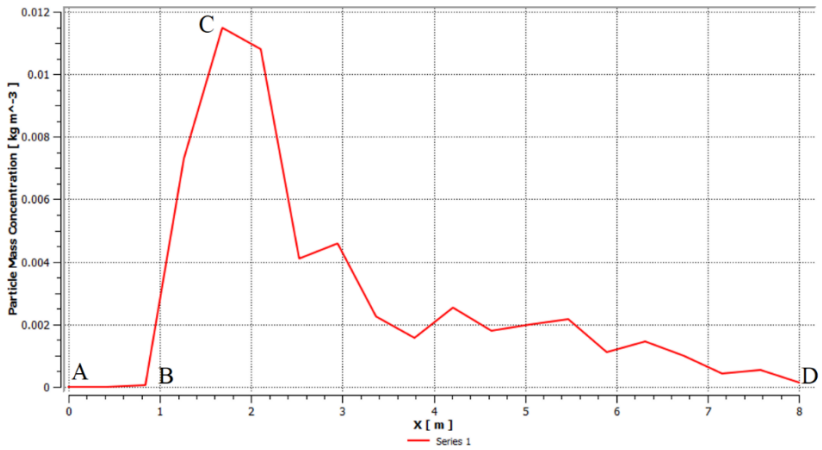

Fig. 4 -The relationship between smoke mass concentration and horizontal distance

Analysis of smoke diffusion temperature field

In order to obtain the space-time variation law of the temperature field in the process of smoke diffusion, the smoke diffusion temperature field at typical moments on the z=0 plane was analyzed. The cloud chart of the smoke diffusion temperature on the z=0 plane is shown in Figure 5(a)~(h). It can be seen from Figure 5 that in a low-temperature environment of 271.15 k (-2 ℃), the high-temperature smoke sprayed from the smoke outlet continuously exchanged heat with the cold air and the temperature of the smoke gradually decreased; High-temperature smoke was mainly concentrated in the center of the plume. As the volume of the plume increased, the temperature at the edge of the plume gradually decreased.

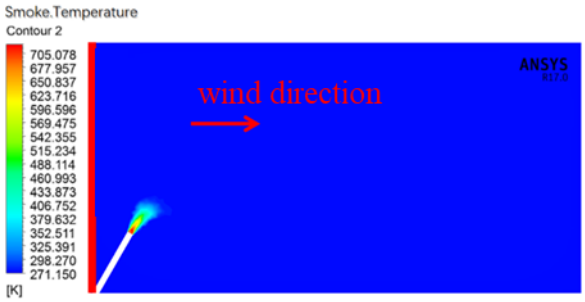

(a) t=1s

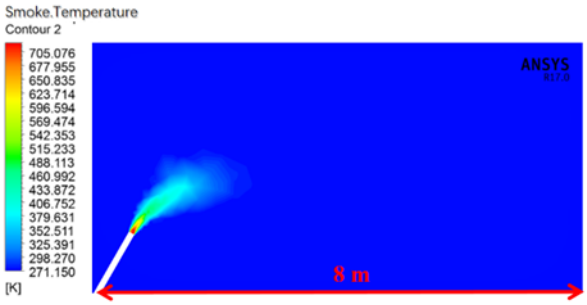

(b) t=3s

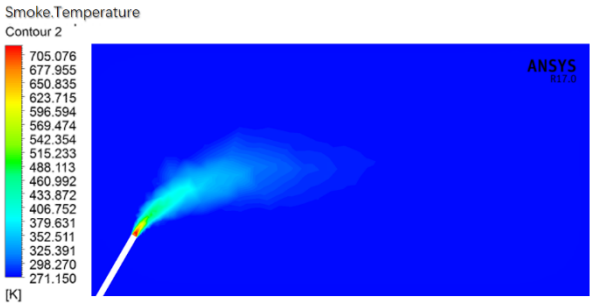

(c) t=5s

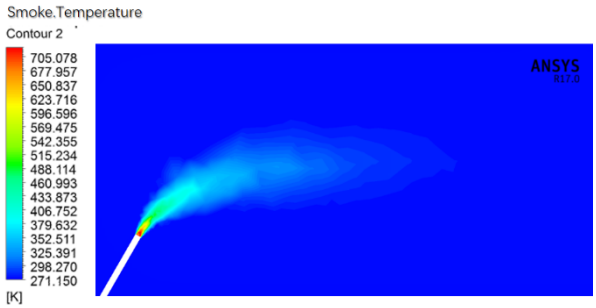

(d) t=7s

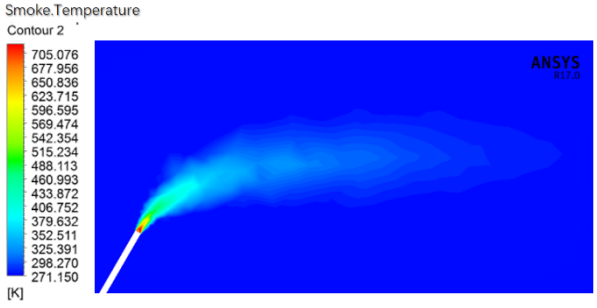

(e) t=9s

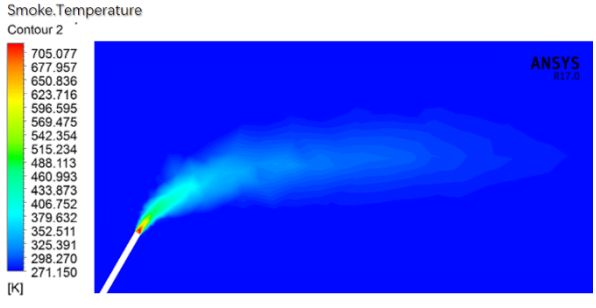

(f) t=11s

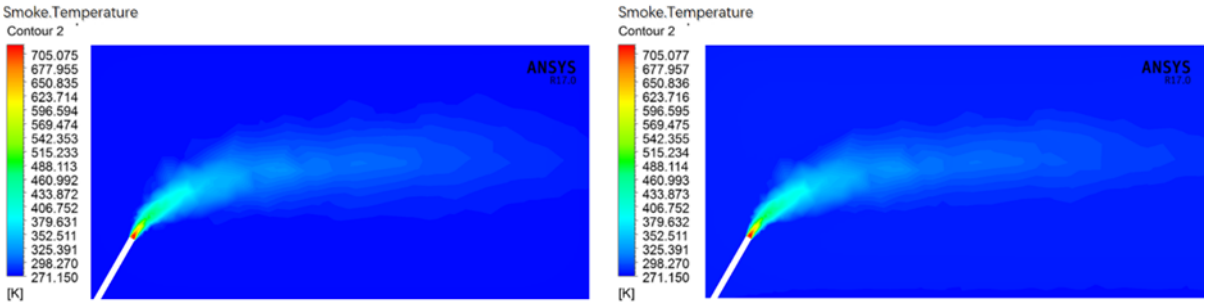

(g) t=13s (h) t=15s

Fig. 5 - Spatial temperature field distribution at different times

By observing the cloud chart of smoke diffusion in Figure 3 and Figure 5, it was found that during the smoke diffusion process, the spatial and temporal distribution characteristics of smoke mass concentration and temperature are basically consistent. In order to further study the spatial and temporal distribution characteristics of the smoke diffusion temperature, the same method as above was used to establish the variation curves of smoke particle temperature with x-axis and y-axis directions, as shown in Fig. 6 and Fig. 7, respectively.

From the variation curve of smoke temperature with x-axis in Fig. 6, it can be seen that during the process of smoke diffusion, the smoke temperature along the x-axis direction showed a sharp increase first and then slowly decreased. The reason for the sharp increase of smoke temperature in BC section is the same as the change of smoke mass con-centration curve. From the variation curve of smoke temperature with the y-axis direction in Fig. 7, it is known that when x=4 m, with the increase of y, the temperature of smoke particles first increased and then decreased, and finally the same as the changing trend of the ambient temperature. It can be seen that the temperature of the smoke particles at the center of the plume is the highest and the temperature gradually decreased as the plume spread from the center to the surroundings, which is consistent with the analysis conclusion in Figure 4. At the same time, it can be seen from the FH section of the curve in Fig. 7 that under certain simulation conditions, the diffusion height of smoke along the y-axis direction is about 2.05 m.

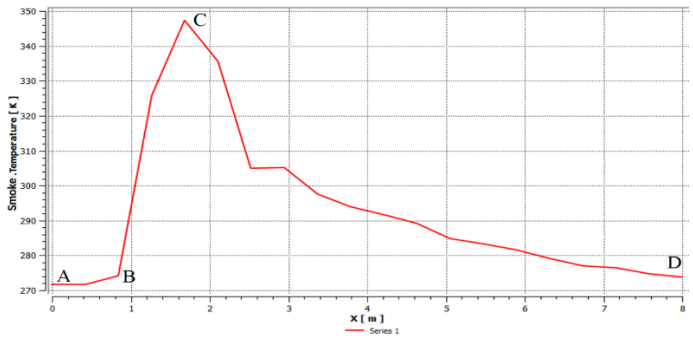

Fig.6 -The relationship between smoke temperature and horizontal distance

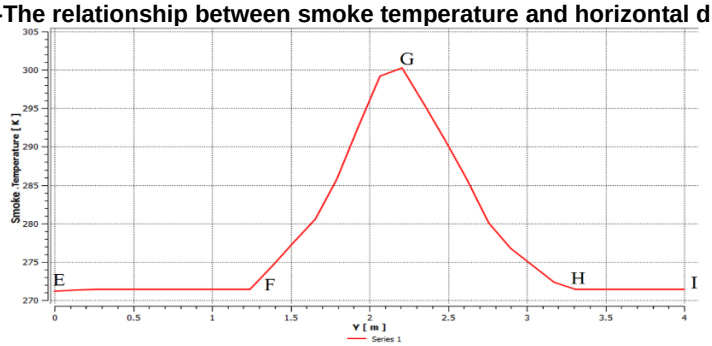

Fig. 7 - The relationship between smoke temperature and vertical distance

Design of orthogonal test

The rapid spread of smoke in a certain area of the orchard is an important measure to improve the anti-frost effect of the orchard. Combined with the structural design of the smoke anti-frost machine in this article, it can be seen that the diffusion effect of the smoke is mainly related to the parameters of the smoke outlet. To study the influence of smoke outlet on the distribution of smoke under different working parameters, the

orthogonal test method was adopted and the velocity of smoke outlet (A), the angle of smoke outlet (B), and the diameter of smoke outlet (C) were taken as the test factors. The level of each factor is three. Taking the warming amplitude near fruit tree canopy (z=0 section, 1.5 m≤y≤3.5 m, 0 m≤x≤8 m) as the index, three factors and three levels of virtual orthogonal experiments were established and the influence of smoke outlet on smoke diffusion under different working parameters was explored.

It can be seen from the overall structure design of the anti-frost machine in hilly orchard that the fan is a key component of the anti-frost machine and the airflow velocity of the smoke outlet has an important influence on the diffusion state of smoke. Low transport efficiency, high transport height, and excessively high or low smoke outlet speed are not conducive to the spread of smoke near the fruit tree canopy. Combined with the actual situation of the northern hilly orchard, it is known that: the velocity of smoke outlet (A) should be 6 m/s~10 m/s, the angle of smoke outlet (B) should be 0 ° ~ 60 ° and the diameter of the smoke outlet (C) should be 60 mm ~ 140 mm. The test Factor Level is shown in Table 2.

Table 2

Test Factor Level of Virtual experiment

Level	Factor		
	(A) The velocity of the smoke outlet（m/s）	(B) The angle of the smoke outlet（°）	(C) The diameter of the smoke outlet（mm）
1	6	0	60
2	8	30	100
3	10	60	140

According to the test factor level in Table 2, orthogonal table L9 (34) was chosen for orthogonal test design. The test scheme is shown in Table 3 and the fourth column in the table is blank.

According to the test data in Table 3, based on the smoke diffusion simulation model, the parameters of simulation model and related boundary conditions were modified and the calculations were finally performed. After the simulation calculation, by collecting and analyzing the data in the CFD-Post post-processing simulation module and filling the obtained data in Table 3 for analysis and calculation, the optimal combination of the primary and secondary order of the factors that affect the warming magnitude and the working parameters was obtained. The orthogonal test design and results are shown in Table 3.

Table 3

Test plan and results

Serial number	Factor				Result Warming magnitude (℃)
	A The velocity of smoke exit (m/s)	B The angle of smoke outlet (°)	C The diameter of smoke outlet (mm)	D (null)	
1	1（6）	1（0）	1（60）	1	0.148
2	1	2（30）	2（100）	2	0.796
3	1	3（60）	3（140）	3	2.043
4	2（8）	1	2	3	0.482
5	2	2	3	1	1.263
6	2	3	1	2	1.329
7	3（10）	1	3	2	0.563
8	3	2	1	3	0.669
9	3	3	2	1	1.989
K_{1j}	2.987	1.193	2.146	3.400	The primary and secondary order of the factors is: BCA The better plan is: $B_3C_3A_1$
K_{2j}	3.074	2.728	3.267	2.688	
K_{3j}	3.221	5.361	3.869	3.194	
k_{1j}	0.996	0.398	0.715	1.133	
K_{2j}	1.025	0.909	1.089	0.896	
K_{3j}	1.074	1.787	1.290	1.065	
R_j	0.078	1.389	0.575	0.237	

Note: K_{1j}, K_{2j}, K_{3j} - the sum of data for each factor column corresponding to level (1,2,3); k_{1j}, k_{2j}, k_{3j} - the comprehensive average of the level data of each factor column; R_j - extreme difference

Analysis of Orthogonal Test Results

It can be seen from the data analysis in Table 3 that the minimum value of warming magnitude near the fruit tree canopy is 0.148 °C and the maximum value is 2.043 °C. At the same time, the greater the warming amplitude, the better the diffusion effect of smoke in the canopy of fruit trees. When the warming magnitude is used as the evaluation index, it was found that the primary and secondary order of the three factors affecting the smoke diffusion effect of the fruit tree canopy was (B) the angle of smoke outlet >(C) the diameter of smoke outlet >(A) the velocity of smoke outlet.

In order to obtain the variation trend of warming magnitude near fruit tree canopy with three factors and three levels, the horizontal values of the factors in Table 3 were used as the abscissas and the values of k_{1j}, k_{2j}, and k_{3j} as the ordinates to draw the effect curve between the influencing factors and the warming magnitude near the fruit tree canopy, as shown in Figure 8. Through the variation trend of the curve in Figure 8, it can be intuitively obtained that the optimal level of the working parameters at the smoke outlet of the anti-frost machine is $B_3C_3A_1$ when the warming magnitude is the largest near the fruit tree canopy. That is, when the velocity of smoke outlet is 6 m /s, the angle of smoke outlet is 60° and the diameter of smoke outlet is 140 mm, the warming magnitude is the largest.

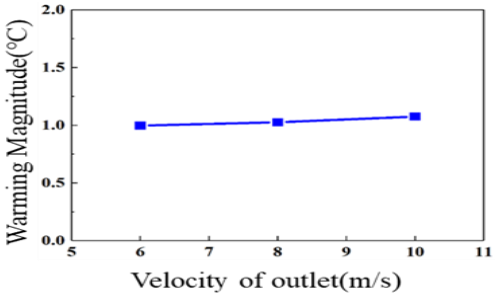

a) Effect curve of the velocity of smoke outlet and warming magnitude

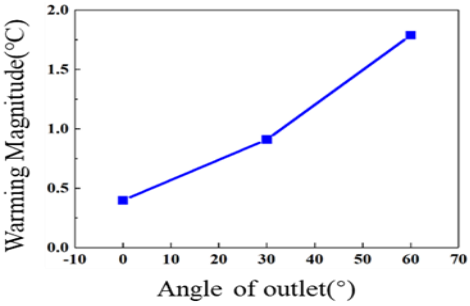

(b) Effect curve of the angle of smoke outlet and warming magnitude

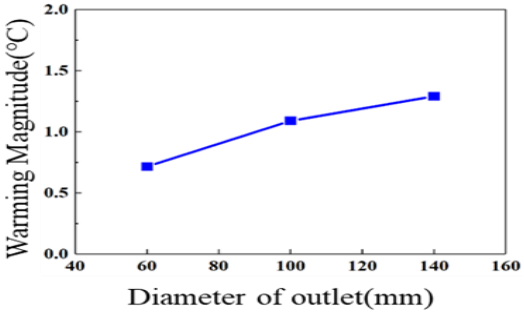

c) Effect curve of the diameter of smoke outlet and warming magnitude

Fig. 8 - Effect curve of influence factors and warming magnitude

It can be seen from the effect curves of Figure 8 (a) ~ (c) that the warming magnitude near the fruit tree canopy is positively correlated with the velocity of smoke outlet, the angle of smoke outlet, and the diameter of smoke outlet. In the process of the velocity of smoke outlet from 6 m/s to 10 m/s, the warming magnitude showed a steady upward trend with the increase of the velocity of smoke outlet. The reason may be that with the gradual increase of the velocity of smoke outlet, the efficiency of smoke delivery increased, but the upward trend was slow. It can be seen that the velocity of smoke outlet had little effect on the warming magnitude near the fruit tree canopy. In the process of the angle of smoke outlet from 0° to 60°, the warming magnitude showed a significant upward trend with the increase of the angle of smoke outlet. The larger the angle of smoke outlet, the greater the temperature increase. The main reason is that with the increase of angle of smoke outlet, the vertical diffusion height of smoke increased, the mass concentration of smoke near the canopy of fruit trees increased and the warming amplitude increased. It can be seen that the angle of smoke outlet had a significant effect on the height of smoke diffusion. In the process of diameter of smoke outlet from 60 mm to 140 mm, the warming magnitude increased with the increase of the diameter of smoke outlet. The main reason is that as the diameter of smoke outlet increased, the efficiency of smoke delivery increased and the velocity of smoke diffusion increased. However, the upward trend of warming magnitude slowed down with the diameter of smoke outlet further increased.

Through the above analysis, the primary and secondary order of the test factors, the optimal combination of working parameters, and the variation trend of the warming magnitude near the fruit tree canopy with the three-factor parameters were obtained. It is impossible to accurately explain the importance of each factor on the test results by range analysis and effect curve analysis. Therefore, in order to further clarify the significance of the influence of each factor level on the warming amplitude, variances were analyzed based on the orthogonal test data in Table 3 by using statistical software SPSS Statistics 23. The results of variance analysis are shown in Table 4.

Table 4

Analysis of variance

Index	Origin	Degree of freedom df	Quadratic	Mean square	F	Significance
Warming amplitude	Modified model	6	3.481	0.580	12.968	0.073
	Intercept	1	9.573	9.573	213.940	0.005
	A	2	0.009	0.005	0.104	0.906
	B	2	2.962	1.481	33.102	0.029
	C	2	0.510	0.255	5.696	0.149
	Error	2	0.089	0.045		
	Total	9	13.144			
	Total after correction	8	3.571			

Note: 1 - The square of R = 0.975 (the square of adjusted R = 0.900); 2- When P <0.01, the degree of influence is extremely significant, when 0.01 <P <0.05, the degree of influence is significant, and when P >0.05, the degree of influence is insignificant

It can be seen from the results of the variance analysis in Table 4 that the angle of smoke outlet has a significant impact on the warming magnitude near the fruit tree canopy and the velocity of smoke outlet has no significant effect on the warming magnitude. It can be seen from the significant results of the variance analysis that the order of the influence of each factor on the warming magnitude near the fruit tree canopy is (B) the angle of smoke outlet > (C) the diameter of smoke outlet > (A) the velocity of smoke outlet. The results of variance analysis are consistent with those of range analysis.

Therefore, an adjusting device for angle at the smoke outlet should be designed. Properly increasing the angle of smoke outlet can increase the height of smoke diffusion and improve the efficiency of smoke diffusion near the fruit tree canopy. In view of the fact that the diameter of smoke outlet and the wind velocity have little influence on the smoke diffusion height, the delivery efficiency of smoke can be increased by appropriately increasing the wind velocity and diameter of the fan.

Field experiment

After the prototype is completed, it can effectively be tested whether the smoke anti-frost machine can meet the requirements of frost protection and intelligent control in orchard field. At the same time, the structure of the smoke anti-frost machine in hilly orchards should be further optimized based on the results of field test.

Based on the agronomic requirements of frost prevention in hilly orchards, the optimal design of working parameters at the smoke outlet of the anti-frost machine showed that the angle of smoke outlet had a significant effect on the diffusion height of smoke. Therefore, in order to improve the diffusion effect of smoke, it is necessary to increase the angle of smoke outlet and install a height adjustment device at the smoke outlet during the processing of the smoke anti-frost machine. The prototype of smoke anti-frost machine based on hilly orchard transport track is shown in Figure 9.

The test site is the horticulture experimental station of the south campus of Shandong Agricultural University, and the test time is January 18, 2022. The height of fruit trees in the orchard is relatively high, the height of the fruit tree canopy is generally concentrated in 3~4 m, the spacing of fruit trees is 1~1.5 m and the row spacing of fruit trees is 3~4 m.

The supporting power of the prototype adopts a remote-controlled hilly orchard track tractor. The smoke-generating and conveying parts are hauled and operated by the tractor. The transportation track is a key component for the mobile operation of the prototype. During the installation process, it is necessary to determine the appropriate track position by observing the topographic features of the orchard.

When installing the track, it is necessary to ensure that the track plane is parallel to the ground, which is conducive to the stable operation of the prototype. After the track installation is completed, the track tractor and smoke-generating and conveying parts of hilly orchard were imported into the track and the prototype was debugged. The situation of orchard and the prototype of smoke anti-frost machine are shown in Figure 9.

Fig. 9 - Hilly orchard frost protection smoke machine

Analysis of test content and result

The frost protection principle of the smoke anti-frost machine showed that the smoke generated by the anti-frost machine can float for a long time to form a smoke layer in the air at a certain height, which effectively reduced the heat radiation loss of soil and fruit trees. At the same time, a large amount of smoke generated by the smoke generation agent dissolved the wet and cold air in the frost orchard into water and released certain latent heat, which effectively improved the temperature of the surrounding environment and achieved the purpose of orchard frost prevention. In order to explore the anti-frost effect of the smoke anti-frost machine, a comparative experiment was carried out on frost prevention effect by taking the warming magnitude of the orchard as the evaluation index after the anti-frost machine worked for 0.5 hours, the frost machine operating orchard as the work area and the non-operating orchard as the contrast area. The working area and the comparison area of the orchard are both 667 m^2.

Before the start of the experiment, 24 temperature monitoring points were set up in the contrast area and the work area respectively, and a temperature recorder was placed at a height of 1.5 ~ 4 m from the ground. The installation position of some RC-4 temperature recorders is shown in Figure 10.

Fig. 10 - Installation of RC-4 temperature recorder

As shown in Figure 11 (a), the orchard smoke anti-frost machine and control button was started to control the prototype to run continuously along the orchard track by using remote controller. As shown in Figure 11(b), all temperature recorders in the work area and the contrast area were started and the temperature changes in the orchard were recorded when the smoke in the work area of the orchard was sufficiently diffused.

(a) Start anti-frost machine (b) Anti-frost machine operation in the orchard

Fig. 11- Hilly orchard frost protection smoke machine operation

After the test, all the data monitored by the temperature recorder were exported and sorted out. The comparison result of the temperature space-time distribution of the comparison area and the work area was obtained by using the grid data interpolation function method, as shown in Figure 12. It can be seen from Figure 12 (a) that before the start of the experiment, the temperature of the orchard in the contrast area was -1.6℃. As time went by, the temperature of the orchard in the contrast area began to gradually decrease. After 0.5 h, the temperature of the orchard in the contrast area dropped to -2.2℃ and the temperature in the contrast area dropped by 0.6℃ within 0.5 h. It can be seen from Figure 12 (b) that the initial temperature is -1.5℃ when the smoke fully diffused in the work area and the temperature in the work area did not change significantly when the anti-frost machine worked for 0.3 hours. With the further increase of the working time of the anti-frost machine, the temperature of the orchard began to show an obvious upward trend. After the anti-frost machine worked for 0.5 hours, the temperature in the work area increased by 1.7℃. The heating effect was relatively significant.

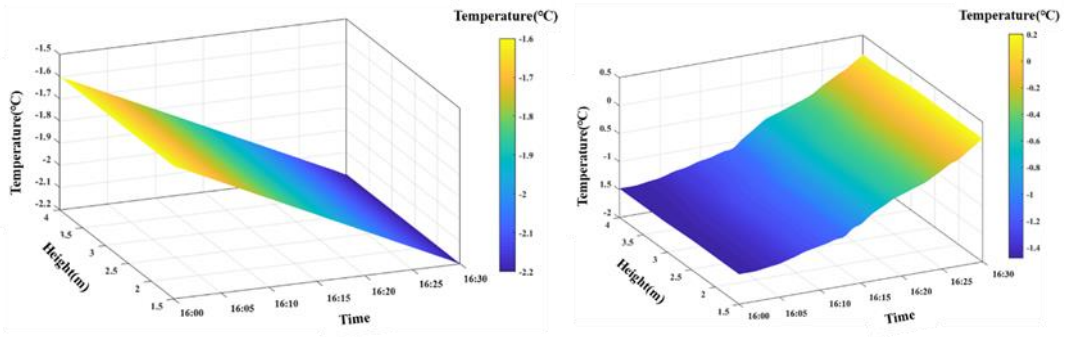

(a) Orchard test comparison area (b) Orchard test working area

Fig. 12 - Temporal and spatial distribution of temperature at different heights in the contrast area and the work area

It can be seen from the result analysis of the above comparative test that the prototype can effectively improve the temperature within the height range of 1.5 m ~ 4 m in the work area. After continuous operation for 0.5 h, the prototype can increase the temperature of the work area by 1.7 °C, which can provide effective protection against orchard frost. However, since the temperature rise in the orchard is relatively slow during the smoke anti-frost operation, when carrying out frost prevention operations in orchards, the smoke anti-frost machine should be opened in advance before the orchard temperature drops to the critical value of frost temperature to improve the anti-frost effect of orchards.

After the operation of the anti-frost machine, the orchard smoke gradually spread, and a thicker smoke screen can be formed at the height of 1.5 to 3 m in the orchard, as shown in Figure 13. The production of the smoke layer can effectively slow down the descending speed of cold air and reduce the heat radiation loss of soil and plants. The smoke layer has the effect of heat preservation, which can provide effective protection for orchard frost. At the same time, according to the actual requirements, the operation time of the smoke anti-frost machine can be adjusted to effectively reduce the cost.

Fig. 13 - Orchard smoke layer effect

CONCLUSIONS

In order to improve the mechanized anti-frost operation of hilly orchards, a smoke anti-frost machine was designed based on the transportation track of hilly orchard by using computer numerical simulation and electronic control technology. The main work and conclusions of this paper are as follows:

(1) The fluid dynamics simulation was established by Fluent, and the diffusion process of smoke was simulated and analyzed based on the discrete phase model. The simulation results showed that smoke erupted continuously at a speed of 6 m/s from the exit and gradually spread horizontally due to the influence of the wind direction. Within 1 ~ 7 s, the volume of the plume increased gradually and the plume had an inverted V-shaped. After 9 s, the smoke reached a stable diffusion state. During the diffusion process, high-temperature smoke was mainly concentrated in the center of the plume. As the volume of the plume increased, the smoke continuously exchanged heat with the cold air and the temperature of the smoke gradually decreased to the ambient temperature.

(2) Using the orthogonal test method, the virtual orthogonal test of three factors and three levels was carried out on the working parameters of the smoke outlet of the anti-frosting machine, which affected the smoke diffusion. The primary and secondary order of the three factors affecting the canopy temperature increase of fruit trees was obtained: the angle of smoke outlet > the diameter of smoke outlet > the velocity of smoke outlet. When the warming magnitude near the fruit tree canopy is the largest, the best combination of working parameters at the smoke outlet is that the velocity of smoke is 6 m/s, the angle of smoke outlet is 60° and the diameter of smoke outlet is 140 mm. At the same time, the influence of working parameters at smoke outlets on smoke diffusion should be further explored and theoretical support for the structural design of smoke outlets should be provided.

(3) Field experiments showed that the prototype was running stably. When the prototype worked continuously at a speed of 0.6 m / s for 0.5 h, the temperature within the height range of 1.5 to 4 m in the work area could be increased by about 1.7°C. The anti-frost machine can form a thick smoke layer at the height of 1.5~3 m in the orchard, which can provide better frost protection and improve the economic benefits of orchards.

ACKNOWLEDGEMENT

This work was sponsored by National key research and development "13th Five Year Plan" project (2016YFD0701701); Shandong modern agricultural industrial technology system - special fund for fruit innovation team (SDAIT-06-12) - special fund for fruit facilities, machinery and equipment post.

REFERENCES

[1] Augspurger, C.K., (2013). Reconstructing patterns of temperature, phenology, and frost damage over 124 years: Spring damage risk is increasing. *Ecology*, Vol. 94, pp.41-50.

[2] Battany, M.C., (2012). Vineyard frost protection with upward-blowing wind machines. *Agricultural and Forest Meteorology*, Vol.157, pp.39-48.

[3] Beyá-Marshall, V., Herrera, J., Santibáñez, F., et al., (2019). Microclimate modification under the effect of stationary and portable wind machines. *Agricultural and Forest Meteorology*, Vol.269-270, pp.351-363.

[4] Dai, Q.I., Zhang, S.B., Li, P.P., Hu, Y.G., (2009). Frost Protection Effects and Control of Wind Machine for Tea Garden under Temperature Inversion during Early Spring (茶园高架风扇防霜效果试验与控制系统设计). *Agricultural technology and equipment*, pp.34-37.

[5] Delagarmmatikas, G., Tsimas, S., (2010). Grinding process simulation based on Rosin-Rammler equation. *Chemical Engineering Communications*, Vol.191, pp.1362-1378.

[6] Ferrez, J., Davison, A.C., Rebetez, M., (2011). Extreme temperature analysis under forest cover compared to an open field. *Agricultural and Forest Meteorology*, Vol.151, pp.992-1001.

[7] González-Tello, P., Camacho, F., Vicaria, J. M., González, P. A, (2008). A modified Nukiyama–Tanasawa distribution function and a Rosin–Rammler model for the particle-size-distribution analysis. *Powder Technology*, Vol.186, pp.278-281.

[8] Hu, Y.G., Liu, S.Z., Wu, W.Y., Wang, J.Z., Shen, J.W., (2015). Optimal flight parameters of unmanned helicopter for tea plantation frost protection. *International Journal Agricultural and Biological Engineering*, Vol.8, pp.50-57.

[9] Jian, L.A., Ji, A., Zw, A., et al, (2020). Practical tracking control with prescribed transient performance for Euler-Lagrange equation – Science Direct. *Journal of the Franklin Institute*, Vol.357, pp.5809-5830

[10] Li, C.F., Dong, Z., Qin, S.J., Zhao J.X., (2018). Occurrence and prevention of orchard frost (果园霜冻的发生与预防). *Anhui Agricultural Science Bulletin*, Vol.24, pp.47-48+90.

[11] Liu, H., (2018). Research on rack tooth forms of self-propelled monorail mountain orchard transporter (自走式单轨道山地果园运输机轨道齿条齿形研究). *Huazhong Agricultural University*.

[12] Mikio, F., Shinsuki, A., (2007). Frost prevention fan apparatus having automatic folding type neck mechanism: JP, JP2007000096.

[13] Poling, E.B., (2008). Spring cold injury to winegrapes and protection strategies and methods. *HortScience A Publication of the American Society for Horticultural Science*, 2008, Vol.43, pp.1652-166.

[14] Ran, K., Wang, H.W., Wei, S.W., et al., (2020). Investigation Report on Freezing Injury of Pear in Midwestern Shandong Province (山东中西部梨产区幼果期冻害调研报告). *Fruit Growers' Friend*, Vol.216(05), pp.12-14+50.

[15] Reese, R.L., Gerber, J.F., (1969). Empirical description of cold protection provided by a wind machine. *J Amer Soc Hort Sci*.

[16] Song, J.F., Hu, X.F., (2017). A mathematical model to calculate the separation efficiency of streamlined plate gas-liquid separator. *Separation and Purification Technology*, Vol.178.

[17] Song, Y.P., Zhang H.M., Gao D.S., Ren L.L., Zhang Z.H, Geng X.Y., (2019). Development status and trend of domestic orchard transportation machinery in hilly and mountainous areas (国内丘陵山地果园运输机械发展现状与趋势). *Journal of Chinese Agricultural Mechanization*, Vol.40, pp.50-55+67.

[18] Vincent W.J. Heusinkveld, J. Antoon van Hooft, Bart Schilperoort, Peter Baas, Marie-Claire ten Veldhuis, Bas J.H. van de Wiel, (2020). Towards a physics-based understanding of fruit frost protection using wind machines. *Agricultural and Forest Meteorology*, Vol. 282–283.

[19] Yan, J.M., G, R., Z, W., et al, (2023). Development and application of hilly and mountainous bamboo monorail transporter (丘陵山地竹林单轨运输机研发与应用). *World Bamboo and Rattan Newsletter*, Vol. 21(01), pp.112-115.

[20] Yazdanpanah, H., Stigter, C.J., (2011). Selective inverted sink efficiency for spring frost protection in almond orchards northwest of Isfahan. *Theoretical and Applied Climatology*, Vol.105, pp.27-35.

[21] Zhang, J.D., Liu, Q.M., Chen, X.H., Bi, C.H., Wang, Y.S., (2019). Technical Measures for Preventing Frost in Spring of Orchard in Yimeng Mountain Area (沂蒙山区果园春季防霜冻技术措施). *Bulletin of Agricultural Science and Technology*, pp.338-339+350.

[22] Zhang, Q., Wang, W., Liao J.A., (2016). Study the status of fertilizing and ditching machines in orchards at home and abroad (国内外果园施肥开沟机的研究现状). *Journal of Agricultural Mechanization Research*, Vol.38, pp. 264-268.